Technical note

A device for characterising the mechanical properties of the plantar soft tissue of the foot

D. Parker [a],*, G. Cooper [b], S. Pearson [a], G. Crofts [a], D. Howard [c], P. Busby [d], C. Nester [a]

[a] School of Health Sciences, University of Salford, UK
[b] School of Engineering, Manchester Metropolitan University, UK
[c] School of Computing, Science & Engineering, University of Salford, UK
[d] College of Science & Technology, University of Salford, UK

ABSTRACT

The plantar soft tissue is a highly functional viscoelastic structure involved in transferring load to the human body during walking. A Soft Tissue Response Imaging Device was developed to apply a vertical compression to the plantar soft tissue whilst measuring the mechanical response via a combined load cell and ultrasound imaging arrangement. Accuracy of motion compared to input profiles; validation of the response measured for standard materials in compression; variability of force and displacement measures for consecutive compressive cycles; and implementation in vivo with five healthy participants. Static displacement displayed average error of 0.04 mm (range of 15 mm), and static load displayed average error of 0.15 N (range of 250 N). Validation tests showed acceptable agreement compared to a Houndsfield tensometer for both displacement (CMC > 0.99 RMSE > 0.18 mm) and load (CMC > 0.95 RMSE < 4.86 N). Device motion was highly repeatable for bench-top tests (ICC = 0.99) and participant trials (CMC = 1.00). Soft tissue response was found repeatable for intra (CMC > 0.98) and inter trials (CMC > 0.70). The device has been shown to be capable of implementing complex loading patterns similar to gait, and of capturing the compressive response of the plantar soft tissue for a range of loading conditions in vivo.

1. Introduction

Plantar soft tissues transfer forces to the skeleton without inducing shock loading or vibration [1,2]. To understand the relationship between plantar tissue structure and function, and inform intervention use when function is lost (e.g. in diabetes, aging [3]), the tissue properties must be characterised under functionally relevant conditions (i.e. in-gait).

In-vitro studies allow the use of accurate materials testing devices for characterisation of whole segment or isolated tissue properties [4], it is however likely that the inherent material properties of the tissues are changed, as a result of tissue breakdown, postmortem.

In-vivo *studies* characterise the tissue in its functional form (e.g. heel pad constrained by skin with regular blood perfusion to venous plexus) [5].

Previous in-vivo methodologies vary in control mechanism and in the accuracy and repeatability achieved for measurement of loading conditions and material deformation. Static measurements of force and tissue compression demonstrate the tissues capacity [6]. Manual or handheld application of compression force is restricted to low rates of displacement (0.6–6 mms^{-1}) and simple patterns of compression (approximately constant rate or sinusoidal) [7,8], neither of which mimic gait conditions. Uncontrolled compression experiments (pendulum and in-gait studies) produce functionally relevant loading but have not captured consecutive compressive cycles [9–11] or have required load and displacement data to be captured separately [12]. Controlled compression experiments (e.g. actuator driven) permit consecutive compressive cycles to be performed in a manner similar to that during walking. Despite this, there has been no attempt to replicate the loading experienced by the heel pad during gait [13,14].

Furthermore the compression surface used has a large effect on the tissue response. Indentation devices result in edge effects [14] and errors can be introduced due to misalignment of the indentation probe [15]. A compression surface larger than the surface area of the segment (heel, forefoot) can ensure uniform loading, free of edge effects, similar to in vivo dynamics [7,13,16,17]. Single axis load cells have been used to capture vertical tissue loading in compression [18], due to their high accuracy and linearity combined with their capacity for high sampling frequency. When uniform compression is applied

Fig. 1. The Soft Tissue Response Imaging Device (STRIDE).

the measured load may not represent a single tissues response. Some in-gait studies have used pressure measurement systems, with a grid of small discrete sensors [11,12], to calculate force over a small region of interest while loading a larger region. Although this provides the potential for greater region specificity, pressure systems are limited by their low sampling frequency and may not reflect the true applied load due to the restricted optimum loading range for these sensors [19]. To overcome these limitations within this study we developed a 2 part loading platen capable of applying uniform loading to the region of interest (heel, forefoot) whilst capturing load measurement via a single axis load cell specific to a central area (heel pad under calcaneus).

To derive both tissue stress and strain, realistic loading must be simultaneous with measurement of tissue displacement. Tissue displacement is measured indirectly in pendulum and indentation studies, and cannot isolate tissue compression from compression/motion of the leg as a whole [20]. Radiology methods permit tissue compression to be measured directly. Fluoroscopy and cineradiography are typically low resolution and restricted to a single layer between the bone and skin surface [21], while ultrasound permits real time image capture combined with high resolution imaging of multiple tissue layers during compression. Ultrasound probes can also be integrated within the compression surface of a loading device [8,22], and combined with load cells to provide synchronous measurement of applied load and tissue thickness [7]. Magnetic Resonance Imaging overcomes these issues [23], but real time dynamic tissue response cannot be measured. Within this study ultrasound was chosen as it permitted effective monitoring of the full compression profile at a high sampling frequency, whilst also enabling measurement of vertical displacement for multiple layers within the plantar tissues.

A device which can apply controlled and uniform tissue compression at high, 'gait like' compression rates is required to provide valid characterisation of plantar soft tissue properties. Therefore the aim of this study was to; (a) develop a device capable of compressing and measuring the plantar soft tissue in a controlled and repeatable manner at a range of compression rates/patterns including those experienced during gait; and (b) evaluate the performance of the device and validate this against a known standard.

2. Methods

2.1. Device design

The Soft Tissue Response Imaging Device (STRIDE) was developed to allow bulk compression of a plantar tissue and region (e.g. heel)

and specific load measurement without inducing edge effects. To achieve this, a bespoke platen was designed (Fig. 1). The platen is divided into two parts; a large aluminium disk (150 mm diameter) with a central hole (32 mm diameter) supported on loadbearing columns, and a central small (30 mm diameter, 6 mm thickness) polypropylene homopolymer sonolucent ultrasound imaging window with 1 mm clearance around its circumference. The probe was coated with ultrasound gel and held in constant contact with the imaging window, a single reverberation artefact was present in the ultrasound image. The central window and the ultrasound probe are connected to the load-cell directly providing an independent load path so that only the force acting on the 30 mm imaging window is measured while compressing the whole foot region.

The platen is mounted on linear bearings and driven by a brushless linear servo-motor (BLMH142, Aerotech Ltd., UK) through a fixed vertical range of ±15 mm making it easy to perform consecutive compression cycles of a specific tissue site (Fig. 2). The device was controlled via displacement, velocity and acceleration input to the
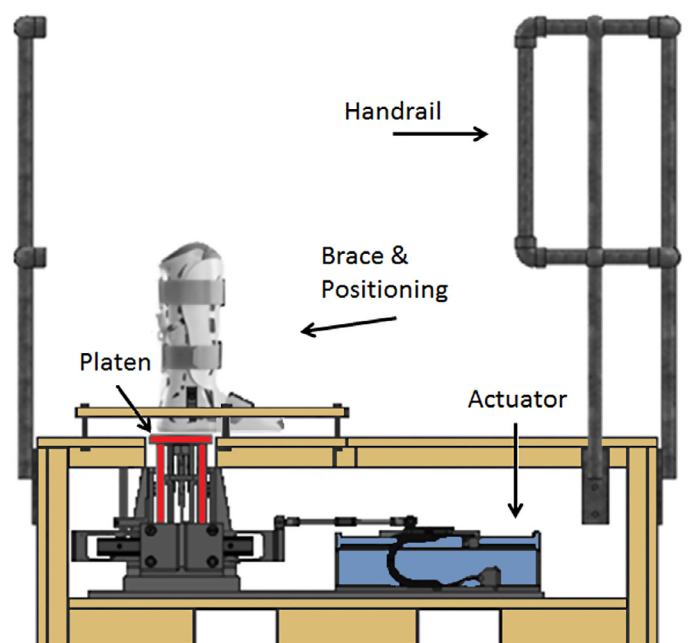
Fig. 2. Cut away view of device housing and brace system.
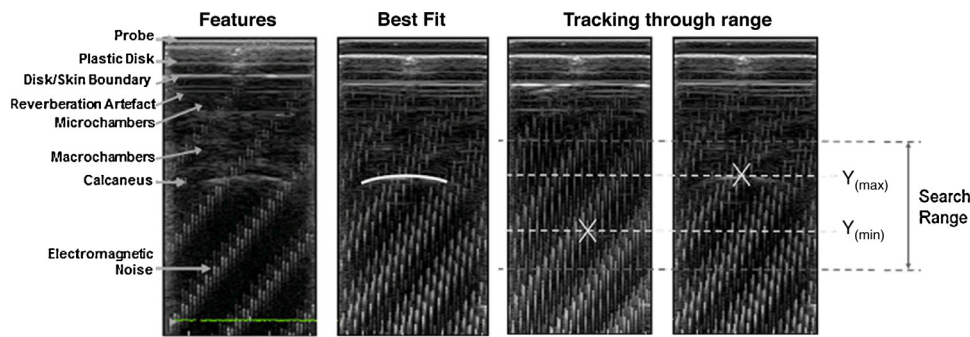
Fig. 3. Ultrasound image of calcaneus demonstrating best fit template and tracking of template through search range to calculate tissue displacement.

supplied drive software (Ensemble, Aerotech Ltd., UK). A Stage was constructed and an Aircast Boot (XP Walker Extra Pneumatic, DJO, LCC, USA) with inflatable bladders was adapted for use as a foot brace to allow positioning directly above the loading platen (Fig. 2). The brace position could be adjusted horizontally and vertically (x, y and z) to permit location of the anatomical site being imaged and thereafter locked. A full health and safety review was conducted to comply with institutional regulations.

2.2. Data collection and processing

The ultrasound system consisted of a 5.5 MHz ultrasound Probe in B-Mode (LA523, MyLab 70, Esaote, Italy) with capture frequency of 201 Hz, capable of imaging the plantar soft tissue to a maximum thickness of 40 mm with a measurement accuracy of 1.75% (± 0.7 mm) as reported by the manufacturer. Ultrasound videos were split into static images (frames) and tissue thickness was determined for each image, using an algorithm written in Python to match an adjustable curve template to the profile of the calcaneal tuberosity (Fig. 3). The distance between the matched template and the skin surface was measured for each image to record tissue thickness over time. A precision load cell with a maximum capacity of 2225 N (TC34, Amber Instruments, UK) and linearity of 0.02% (4.45 N) was used to capture the force response of the plantar tissue for a single axis (compression). A Linear Variable Differential Transformer (LVDT) (S-Series, Solartron, UK) with range of 50 mm and linearity of 0.2% (0.1 mm) provided a measurement of the platen's vertical displacement. Data for the load cell and LVDT were synchronously logged to PC at 1000 Hz capture frequency via LabView (National Instruments, UK).

2.3. Drive profiles

Two drive profiles were used; a 5 mms^{-1} Triangle-Wave Profile (T-Wave) and an impact like Vertical Gait Profile (V-Gait) (Visible in Fig. 4). The T-Wave was based on previous low rate, controlled compression experiments [7,14]. The V-Gait was derived from the vertical component of motion capture data for a marker placed on the posterior aspect of the heel and had cycle duration of 1 s. Velocity and acceleration profiles were calculated as the first and second derivatives for the displacement profile. A peak velocity of 0.6 m/s and a peak acceleration of 15 m/s^2 occurred at the transition peak displacement. These values are much greater than those derived by single Sine-wave fits to the literature data, and it is likely that this is due to the reduced time to peak displacement in the motion capture data (0.05 s) compared to the literature data (0.2 s) [9,24]. This produced a loading profile similar to previous pendulum and in-gait studies [20,21,24]; but with a greater degree of control and repeatability, and permitting consecutive compressive cycles to be performed. All profiles included periods of pre/post compression motion to allow adequate

loading/unloading velocities to be achieved at the points of impact and offloading.

2.4. Device evaluation

2.4.1. Calibration

The load cell was calibrated statically using standard weights within the range of operation (0–250 N). These weights were then reapplied to assess the accuracy and linearity of the measured load. To remove the effects of mechanical friction and inertia, created when accelerating the suspended STRIDE platen, dynamic calibration profiles were applied, which were the average cycle load measured for 100 cycles of platen motion in free air. To correct for systematic error in the load cell measurements a secondary correction factor in the form $y = (x - 1.58)^* 1.05$ was applied. The LVDT was calibrated statically using metric gauge blocks for the operational range (0–30 mm). The device was then moved at 3 mm steps through its full range to assess the linearity and accuracy of platen displacement.

2.4.2. Input/output precision

To assess the ability of the drive mechanism and coupling systems to conform to the input drive profile, data for vertical displacement of the device platen was collected using the LVDT (Fig. 4). 100 displacement cycles were run for both drive profiles, in free air and during compression of a standard material (Thermoplastic rubber – Shore 25).

2.4.3. Validation

To validate the force and displacement measurements recorded in compression, material tests were conducted using STRIDE and then repeated on a Houndsfield tensometer (Model H10KS) for two standard materials (Thermoplastic rubber of Shore A25 and A35) selected to match reported hardness values for the plantar soft tissue [25]. Prior to testing the thickness was measured using a digital calliper. The material was then placed into the testing device and a pre-load of 1 N was applied to ensure firm contact. Each material was tested at three displacement velocities (0.5 mms^{-1}, 1 mms^{-1}, 2 mms^{-1}) for 10 cycles of a triangle wave with amplitude of 10 mm. Between tests each material was allowed to return to its original thickness.

2.4.4. In vivo plantar soft tissue testing

To provide an initial assessment of the devices application to in-vivo plantar soft tissue testing the right feet of 5 healthy individuals were tested. The participants were of a similar age and BMI (Table 1), and recruited from the population at the University of Salford. Participants had no history of foot problems or surgery, and no history of systemic pathophysiological disease. Ethical approval was given by the local ethics committee and each participant provided written informed consent. The right leg was braced, and the participant was made to stand , positioned such that the heel and straight leg were directly above the imaging window of the STRIDE platen (Fig. 2). The
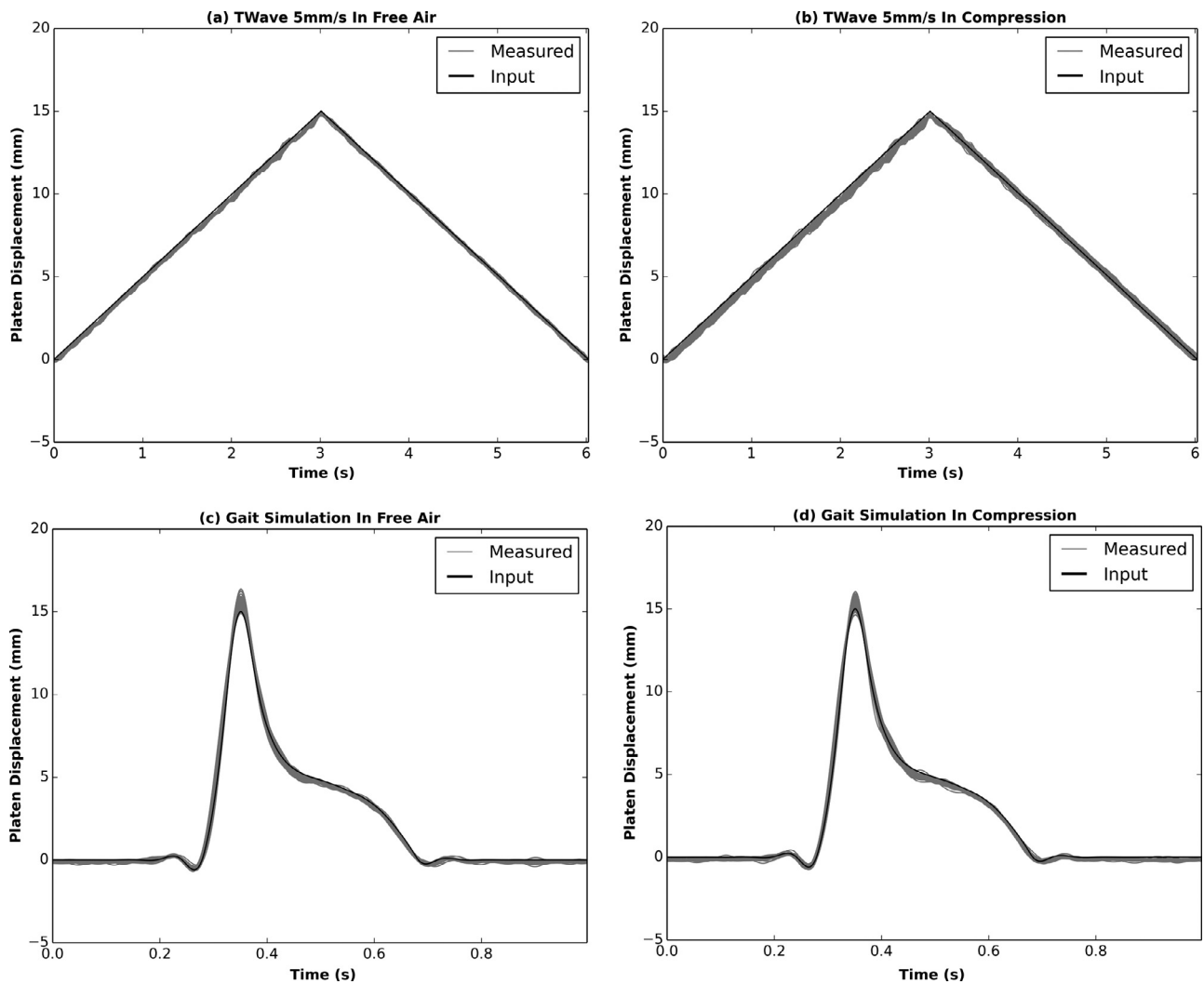
Fig. 4. Input/output precision for platen motion in all conditions.

Table 1
Participant information.

Participant		1	2	3	4	5	Mean ± SD
Age	(yr)	26	24	20	20	25	23.00 ± 2.53
Gender	(m:f)	m	m	f	f	m	3 m/2f
Height	(cm)	181	178	175	172	169	175.00 ± 4.24
Body mass	(kg)	82	78	78	60.9	60	71.78 ± 9.37
BMI	(kg/m^2)	25	24.6	25.5	20.6	21	23.34 ± 2.10
UHP thickness	(mm)	19.34	16.36	18.40	13.42	17.42	16.99 ± 2.04

*UHP – Unloaded HEEL Pad.

STRIDE platen was then brought into contact with the plantar surface of the heel to permit a sagittal plane ultrasound image of the heel fat pad to be obtained and the apex of the calcaneal tubercle imaged. While recording ultrasound images, a small displacement (∼5 mm) was applied to compress the tissue and the platen then lowered until tissue contact was lost. The final image before loss of contact was used to measure unloaded tissue thickness, based on the protocol of Cavanagh (1999). Dynamic tissue tests were conducted as three separate trials, each consisting of two consecutive compressions, resulting in six compressions in total for each loading condition (T-wave, V-Gait). The two compressions in each trial were made in close succession so that small intra-trial differences were expected. However, between trials the tissue was fully offloaded and allowed to recover

to its unloaded state leading to the possibility of larger inter-trial differences.

3. Results

The load cell calibration was linear (Pearson's $R^2 = 0.999$), with a mean absolute error across all points 0.15 N (SD = 0.07 N), representing 0.06% of the operational range, the maximum error was 0.25 N. For the LVDT the calibration was linear (Pearson's $R^2 = 0.999$) and the mean absolute error across all points 0.04 mm (0.02 mm SD), 0.24% of the operational range, and the maximum error was 0.07 mm. The device reproduced input profiles with NRMSE of <1.7% of the displacement range across the whole loading profile (Table 2) and ICC's > 0.99 for all conditions. Errors were highest at the transition from upward to downward motion of the platen which represented the point of greatest acceleration (Fig. 4). The target displacement error, captured at this transition, was <3.4% of the displacement range for all conditions. Absolute measures of target error show that the T-wave trials were consistently below the target, while gait simulation trials consistently exceeded the target (Table 2). Acceptable agreement was found between STRIDE and Houndsfield tensometer for measured displacement in all conditions with an NRMSE < 1.4% for the displacement range (Table 3). However, the measured load displayed a greater variance between the two measurement devices with NRMSE <9% for the measured range (Table 3) the RMSE ranged from 2–5 N

Table 2
Input/output conformance and target error for platen motion.

Input/output conformance		RMSE (mm) Mean ± SD	NRMSE (%)	ICC$_{(1,1)}$
T-Wave 5 mm s^{-1}	In free air	0.181 ± 0.020	1.221	0.999
	In compression	0.241 ± 0.065	1.639	0.999
Gait simulation	In free air	0.223 ± 0.037	1.386	0.999
	In compression	0.209 ± 0.038	1.306	0.999
Target error		RMSE (mm) Mean ± SD	NRMSE (%)	Absolute (mm) Mean ± SD
T-Wave 5 mm s^{-1}	In free air	0.192 ± 0.062	1.294	−0.192 ± 0.062
	In compression	0.307 ± 0.059	2.089	−0.307 ± 0.059
Gait simulation	In free air	0.540 ± 0.270	3.330	0.534 ± 0.281
	In compression	0.399 ± 0.231	2.479	0.366 ± 0.280

Root Mean Square Error (RMSE) calculated by comparing input profile to output cycle measurements. Normalised RMSE (NRMSE) was calculated as the mean RMSE divided by the range of measurement. The error was defined as the discrepancy between the expected position (+15 mm) and the actual position of the device platen, at peak displacement. Absolute error allows identification of over or undershooting of the device platen.

Table 3
Device comparison.

	Displacement			Force		
Stride vs. HT	RMSE (mm) Mean ± SD	NRMSE (%)	CMC	RMSE (N) Mean ± SD	NRMSE (%)	CMC
Shore 25						
0.5 mm s^{-1}	0.173 ± 0.098	0.734	0.998	2.284 ± 0.236	5.372	0.980
1 mm s^{-1}	0.114 ± 0.030	0.593	0.999	3.202 ± 0.273	8.851	0.965
2 mm s^{-1}	0.066 ± 0.014	0.387	1.000	2.352 ± 0.319	5.337	0.983
Shore 35						
0.5 mm s^{-1}	0.118 ± 0.024	0.464	0.999	3.914 ± 0.170	7.228	0.980
1 mm s^{-1}	0.168 ± 0.029	1.392	0.999	2.806 ± 0.271	4.815	0.988
2 mm s^{-1}	0.074 ± 0.027	0.249	1.000	4.851 ± 0.187	8.875	0.974

Root Mean Square Error (RMSE) calculated by comparing the Houndsfield Tensometer (HT) and the Soft Tissue Response imaging device (STRIDE). Normalised RMSE (NRMSE) was calculated as the mean RMSE divided by the range of measurement. The Coefficient of Multiple Correlations (CMC) was used to assess the level of agreement for the two dimensional curve data of the two device outputs [37].

Table 4
Variation in measured compressive response during participant tests.

		NRMSE (%)		% CV		CMC	
Output measure		Intra	Inter	Intra	Inter	Intra	Inter
5 mm s^{-1} T-wave							
	Platen motion	0.115	0.078	0.23 ± 0.04	0.16 ± 0.02	1.000 ± 0.000	1.000 ± 0.000
	US displacement	1.942	5.198	6.29 ± 1.33	18.17 ± 7.63	0.988 ± 0.009	0.706 ± 0.126
	Load measurement	1.539	4.046	4.15 ± 1.33	11.30 ± 3.66	0.996 ± 0.001	0.834 ± 0.094
Gait simulation							
	Platen motion	0.101	0.1	0.69 ± 0.13	0.73 ± 0.26	1.000 ± 0.000	1.000 ± 0.000
	US displacement	0.952	2.736	11.04 ± 5.19	35.29 ± 19.52	0.992 ± 0.006	0.854 ± 0.061
	Load measurement	0.892	3.894	10.18 ± 5.59	45.71 ± 8.66	0.994 ± 0.004	0.838 ± 0.092

US – Ultrasound, Normalised Root Mean Square Error (NRMSE) was calculated as the mean RMSE between the individual cycle response and the mean response for all cycles divided by the range of operation. Coefficient of Variation (CV) was calculated to provide an assessment of the total variability and represents the width of the SD band in percentage terms [38]. The Coefficient of Multiple Correlations (CMC) was used to assess the level of agreement for the two dimensional curve data of the two device outputs [37].

across the whole load deformation curve. For both load and displacement in all conditions CMC values were high (>0.95). Platen motion was highly repeatable during tissue compression, for both the intra- and inter-trial assessment (NRMSE < 0.11%; CMC > 0.99) in both T-Wave and V-Gait conditions (Table 4, Fig. 5). Measures of tissue compression derived from ultrasound imaging had acceptable repeatability intra trial (NRMSE < 1.95%; CMC > 0.98), however a greater variance was observed inter trial (NRMSE < 5.2%; CMC > 0.70) (Table 4, Fig. 5). The measured load was reasonably repeatable with inter-trial variance (NRMSE < 4.1%; CMC > 0.83) being greater than intra trial variance (NRMSE < 1.6%; CMC > 0.99) for both T-Wave and V-Gait Conditions (Table 4, Fig. 5).

4. Discussion

4.1. Device development

The level of control and range of profiles which can be accurately implemented using STRIDE represents a clear advance from previous in-vivo methods of controlled compression. These were limited
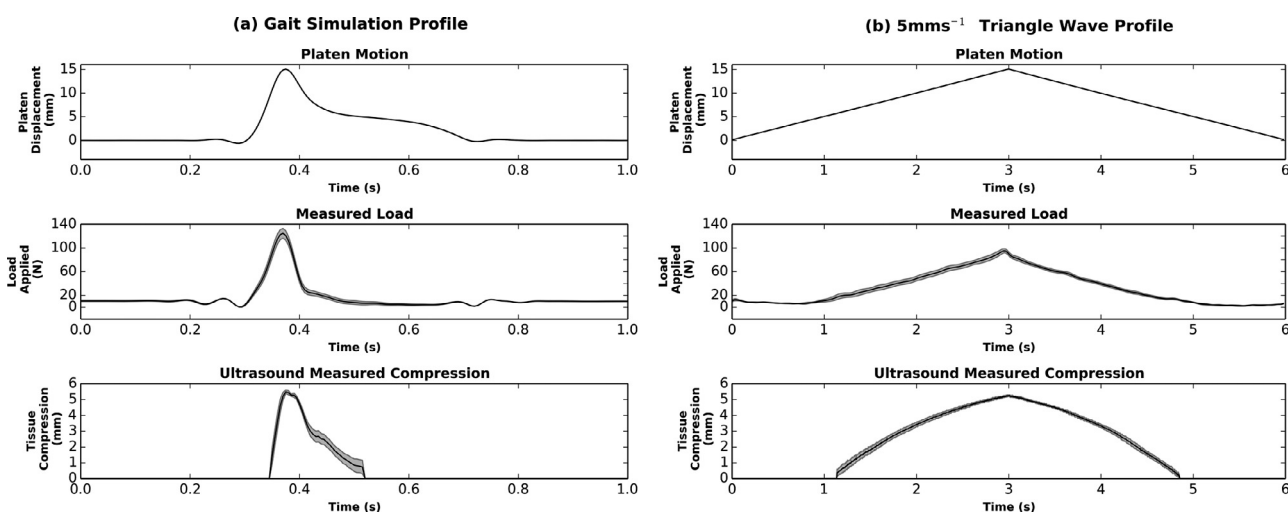
Fig. 5. Platen moion, measured load and ultrasound measured thickness during participant testing for (a) Gait-Sim and (b) Twave profiles based on mean and SD of 6 cycles from 3 Trials for a representative subject.

to simple compression profiles [26–28] or uncontrolled impact style conditions [5,20]. The increased control permitted use of a V-Gait profile which closely reflects the velocities and displacements seen in gait, whilst also enabling capture of the tissues response for consecutive compressive cycles.

The previously demonstrated methods for isolation of tissue specific characteristics have been limited by the inclusion of edge effects resulting in unrealistic tissue compression [14,15,29]. Therefore, the compressive platen of STRIDE was developed to permit bulk compression of the tissue (as per gait) whilst retaining high regional specificity. This unique feature allows for effective recording of phenomena such as stress concentrations, which occur beneath the bony prominences in the foot, during compression [30,31]. For the calcaneus, the region of tissue which lies directly beneath the calcaneal tubercle will receive the greatest compressive force, due to the concentrated stress, while the regions surrounding this will receive a lesser distributed force [31]. It is therefore necessary to isolate the response of the tissue in this region. The use of ultrasound in series with region specific load measurement also provides the capacity to accurately measure tissue strain and stress synchronously, specific to a region of interest.

The device setup provides only a single axis of motion and thus compression imposed by the STRIDE platen represents a simplified version of gait dynamics. To limit the effect of the simplified dynamics vertical motion was selected, as this represents the major compressive component of gait. The device bracing was shown to be compliant during tissue compression, which prevents over compression of the foot; however this compliance is also likely to have resulted in sub-maximally compressed tissue. Compression or strain error have previously been shown to considerably affect the measured peak stress and thus care should be taken when comparing between trials with variable peak strain [32].

4.2. Device performance

Accuracy was within the range reported previously [22,28,29]. Input/output precision tests demonstrated that the device has an average displacement error of 0.225 mm (1.5% for 15 mm range) for compressive trials. This is not as good as the average accuracy reported previously [28,29], but in these studies displacement velocities were much lower than the present study, which attempted to replicate functional loading [33] (0.5–30 mms^{-1}, compared to 5 mms^{-1} – peaks of 300 mms^{-1}). For the V-Gait profile in free-air absolute target error was positive suggesting over compression would occur during

tissue trials. However this error was reduced during material compression trials and it is expected that the impact of the platen with the material reduces actuator work resulting in improved agreement to the input profile. Even so to ensure safety during participant trials the bracing system was designed to be slightly compliant and permit quick release, reducing risk of over compression of the foot.

STRIDE was shown to be capable of replicating the motion of the Houndsfield tensometer with minimal differences (NRMSE < 1.4%) for all conditions meaning the materials were subjected to equal test conditions. Differences were observed between devices for the measured load response (2–5 N RMSE), which suggests some limitations to the capacity to measure the load response accurately with STRIDE. A large component of this error is expected to be the effect of load cell accuracy ($\pm$4.45 N) for the narrow testing range used (0–50 N). However the CMC values were still very high (>0.95) suggesting a consistent pattern of response was seen with both devices (Table 4). The Houndsfield tensometer was only capable of reproducing simple loading profiles with velocities lower than that achievable using STRIDE, as such a validation of the V-Gait Sim profile was not possible.

The high levels of repeatability of platen motion during in-vivo tissue testing, for both T-Wave and V-Gait profiles, confirms the capacity of STRIDE to perform tissue compression at a functionally relevant level (Fig. 5). Combined with the high temporal resolution available with STRIDE, this device offers an opportunity to fully explain the rate dependent nature of the plantar soft tissue in-vivo. High Intra trial repeatability was observed for the response measures (load and tissue compression), within the range of previous studies which assessed cycle to cycle variance [15,34], and sufficient to measure the force displacement response of the tissue in compression. Within day, inter trial the observed variance was greater which may be the result of participant repositioning between trials, or foot motion within the brace system during the dynamic compressive tests. However, this increased variance (~5%) was still within the range observed in previous studies [22,28]. Participant movement during the pre/post compression phases may have affected tissue compression, however the peak tissue compression (~6 mm ~0.3 strain) achieved for both loading profiles is within the range observed for previous studies [21,24,35].

The biomechanical assessment of the plantar tissue has primarily focussed on the vertical response, and does not assess horizontal forces associated with bulging of the heel pad [11,18]. This bulging is a result of the heel pads fibrous septae which create enclosed chambers, acting as hydrostats under compression [36], As the vertical

compressive limit is reached the fibro-elastic septae becomes the dominant resistive force [11]. The use of ultrasound imaging within STRIDE permits tracking of this horizontal movement and warrants further investigation to understand the physiological limits of this tissue.

The capacity to apply bulk compression of tissue (as per gait), whilst retaining high regional specificity, permits effective load and tissue thickness measurement, with acceptable repeatability across all measurements (NRMSE < 5.2%). This enables participant specific characterisation of tissue properties in compression using STRIDE.

Funding

Ethical approval

Ethical approval was given by the University of Salford ethical review panel.

Conflict of interest

The authors of this manuscript have no conflict of interest relevant to this work.

Acknowledgements

References

[1] Alexander RM, Bennett MB, Ker RF. Mechanical properties and function of the paw pads of some animals. J Zool 1986;209:405–19.

[2] Noe DA, Voto SJ, Hoffmann MS, Askew MJ, Gradisar IA. Role of the calcaneal heel pad and polymeric shock absorbers in attenuation of heel strike impact. J Biomed Eng 1993;15(1):23–6.

[3] Kwan RL-C, Zheng Y-P, Cheing GL-Y. The effect of aging on the biomechanical properties of plantar soft tissues. Clin Biomech 2010;25(6):601–5.

[4] Aerts P, Ker RF, De Clercq D, Ilsley DW. The effects of isolation on the mechanics of the human heel pad. J Anat 1996;188(2):417–23.

[5] Weijers R, Kessels A, Kemerink G. The damping properties of the venous plexus of the heel region of the foot during simulated heelstrike. J Biomech 2005;38(12):2423–30.

[6] Zheng YP, Huang YP, Zhu YP, Wong M, He JF, Huang ZM. Development of a foot scanner for assessing the mechanical properties of plantar soft tissues under different bodyweight loading in standing. Med Eng Phys 2012;34(4):506–11.

[7] Hsu C-C, Tsai W-C, Hsiao T-Y, Tseng F-Y, Shau Y-W, Wang C-L, Lin S-C. Diabetic effects on microchambers and macrochambers tissue properties in human heel pads. Clin Biomech 2009;24(8):682–6.

[8] Tong J, Lim CS, Goh OL. Technique to study the biomechanical properties of the human calcaneal heel pad. Foot 2003;13(2):83–91.

[9] Cavanagh PR. Plantar soft tissue thickness during ground contact in walking. J Biomech 1999;32(6):623–8.

[10] Rome K, Campbell RS, Flint AA, Haslock I. Ultrasonic heel pad thickness measurements: a preliminary study. Br J Radiol Nov. 1998;71(851):1149–52.

[11] Wearing SC, Hooper SL, Dubois P, Smeathers JE, Dietze A. Force–deformation properties of the human heel pad during barefoot walking. Med Sci Sports Exerc 2014;46(8):1588–94.

[12] Telfer S, Woodburn J, Turner DE. An ultrasound based non-invasive method for the measurement of intrinsic foot kinematics during gait. J Biomech 2014;47(5):1225–8.

[13] Aerts P, Ker RF, De Clercq D, Ilsley DW, Alexander RM. The mechanical properties of the human heel pad: a paradox resolved. J Biomech 1995;28(11):1299–308.

[14] Erdemir A, Viveiros ML, Ulbrecht JS, Cavanagh PR. An inverse finite-element model of heel-pad indentation. J Biomech 2006;39(7):1279–86.

[15] Zheng Y-P, Mak AF, Lue B. Objective assessment of limb tissue elasticity: development of a manual indentation procedure. J Rehabil Res Dev 1999;36(2):71–85.

[16] Ker RF. The time-dependent mechanical properties of the human heel pad in the context of locomotion. J Exp Biol 1996;199(7):1501–8.

[17] De Clercq D, Aerts P, Kunnen M. The mechanical characteristics of the human heel pad during foot strike in running: an in vivo cineradiographic study. J Biomech 1994;27(10):1213–22.

[18] Rome K. Mechanical properties of the heel pad: current theory and review of the literature. Foot 1998;8(4):179–85.

[19] Abdul Razak AH, Zayegh A, Begg RK, Wahab Y. Foot plantar pressure measurement system: a review. Sensors 2012;12(7):9884–912.

[20] Alcántara E, Forner A, Ferrús E, García A-C, Ramiro J. Influence of age, gender, and obesity on the mechanical properties of the heel pad under walking impact conditions. J Appl Biomech 2002;18(4):345–56.

[21] Wearing SC, Smeathers JE, Yates B, Urry SR, Dubois P. Bulk compressive properties of the heel fat pad during walking: a pilot investigation in plantar heel pain. Clin Biomech 2009;24(4):397–402.

[22] Rome K, Webb P. Development of a clinical instrument to measure heel pad indentation. Clin Biomech 2000;15(4):298–300.

[23] Petre M, Erdemir A, Cavanagh PR. An MRI-compatible foot-loading device for assessment of internal tissue deformation. J Biomech 2008;41(2):470–4.

[24] Gefen A. In vivo biomechanical behavior of the human heel pad during the stance phase of gait. J Biomech 2001;34(12):1661–5.

[25] Periyasamy R, Anand S, Ammini AC. The effect of aging on the hardness of foot sole skin: a preliminary study. The Foot 2012;22(2):5–99.

[26] Fontanella CG, Forestiero A, Carniel EL, Natali AN. Analysis of heel pad tissues mechanics at the heel strike in bare and shod conditions. Med Eng Phys 2013;35(4):441–7.

[27] Hsu C-C, Tsai W-C, Chen CP-C, Shau Y-W, Wang C-L, Chen MJ-L, Chang K-J. Effects of aging on the plantar soft tissue properties under the metatarsal heads at different impact velocities. Ultrasound Med Biol 2005;31(10):1423–9.

[28] Xiong S, Goonetilleke RS, Witana CP, Rodrigo WDAS. An indentation apparatus for evaluating discomfort and pain thresholds in conjunction with mechanical properties of foot tissue in vivo. J Rehabil Res Dev 2010;47(7):629–41.

[29] Klaesner JW, Commean PK, Hastings MK, Zou D, Mueller MJ. Accuracy and reliability testing of a portable soft tissue indentor. IEEE Trans Neural Syst Rehabil Eng 2001;9(2):232–40.

[30] Chen W-P, Tang F-T, Ju C-W. Stress distribution of the foot during mid-stance to push-off in barefoot gait: a 3-D finite element analysis. Clin Biomech 2001;16(7):614–20.

[31] Spears IR, Miller-Young JE, Waters M, Rome K. The effect of loading conditions on stress in the barefooted heel pad. Med Sci Sports Exerc 2005;37(6):1030–6.

[32] Pai S, Ledoux WR. The effect of target strain error on plantar tissue stress. J Biomech Eng 2010;132(7):071001.

[33] Parker D. Characterising the biomechanical properties of the plantar soft tissue under the conditions of simulated gait. [Ph.D.]. The University of Salford; 2013.

[34] Jorgensen U. The HPC-device: a method to quantify the heel pad shock absorbency. Foot Ankle 1989;10(2):93–8.

[35] Uzel M, Cetinus E, Ekerbicer HC, Karaoguz A. Heel pad thickness and athletic activity in healthy young adults: a sonographic study. J Clin Ultrasound 2006;34(5):231–6.

[36] Hsu C-C, Tsai W-C, Wang C-L, Pao S-H, Shau Y-W, Chuan Y-S. Microchambers and macrochambers in heel pads: Are they functionally different. J Appl Physiol 2007;102(6):2227–31.

[37] Kadaba MP, Ramakrishnan HK, Wootten ME, Gainey J, Gorton G, Cochran GVB. Repeatability of kinematic, kinetic, and electromyographic data in normal adult gait. J Orthop Res 1989;7(6):849–60.

[38] Winter DA. Kinematic and kinetic patterns in human gait: variability and compensating effects. Hum Mov Sci 1984;3(1–2):51–76.